ELSEVIER

Chemical Engineering Journal 74 (1999) 77–83

Chemical Engineering Journal

Accelerated molecular dynamics of infrequent events

S. Pal, K.A. Fichthorn*

Department of Chemical Engineering and Physics, Pennsylvania State University, University Park, PA 16802, USA

Abstract

Diffusion of molecules in and on solid substrates often occurs as a series of hops between neighboring binding sites, or potential-energy minima. Simulation of this type of transport with molecular dynamics becomes challenging because the time between hops often exceeds times that can typically be probed with this computational technique. In this paper, we discuss a new method, which extends the time scale in molecular-dynamics simulations, while retaining nearly precise dynamic detail. A simple two-dimensional model has been used to explore the algorithm in detail. We also discuss the extension of the method to more complicated system, involving the diffusion of a Ag adatom on the Ag (0 0 1) surface.

Keywords: Molecular-dynamic (MD) simulation; Monte Carlo (MC) simulation; Transition-state theory (TST); Potential-energy surface

1. Introduction

A continuing challenge in materials simulation is to conduct long-time simulations of structural evolution, while accurately retaining atomic detail. Molecular-dynamics (MD) simulations can provide accurate details at the atomic scale; however, they are not practical for simulating times beyond the nanosecond range. In many materials, dynamical evolution occurs through a series of ''rare events'', in which the system spends a long time period in one potential-energy minimum before escaping and moving on to another. Since the localized motion in the potential-energy minima is not significant, dynamical evolution can be simulated as a series of long-time jumps between potential-energy minima. This is the aim of dynamical Monte Carlo (MC) simulations [1–5]. In principle, if a dynamical MC simulation can incorporate all potential-energy minima of a system and the transition-state theory (TST) [6–8] rates of all possible long-time jumps between the potential-energy minima are accurate, then this technique can reach macroscopic times while retaining the accuracy of MD. In practice, however, this is not always possible. For example, in amorphous solids (e.g., glassy polymers, ice, silicon, metals, etc. [9–12]) and heteroepitaxial thin films, it is very difficult and computationally expensive to accurately classify all of the potential-energy minima and the jumps between them. Hence, dynamical MC methods cannot be rigorously applied to these systems and accurate prediction of their long-time dynamical behavior remains a challenge.

Recently, Voter [13] has developed a method for extending the time scale in MD simulations of systems with rare-event dynamics. In this method, the potential-energy surface is altered in such a way that in a MD simulation on the modified surface, less computer time is spent in simulating motion in the potential-energy minima. The key requirement in this method is to devise a modified potential-energy surface that raises the potential energy near the minima with the constraint that the modified potential match the original one near the TST dividing surface. Fulfilment of this constraint guarantees that the probabilities for escape from a given state satisfy detailed balance with various adjacent states. To construct the modified potential-energy surface $V'(\{\mathbf{r}_N\})$, a boost potential $\Delta V_b(\{\mathbf{r}_N\})$ is added to the original potential $V(\{\mathbf{r}_N\})$. Here $\{\mathbf{r}_N\}$ denotes the full set of Cartesian coordinates for the N particles, $\{\mathbf{r}_N\} = \{\mathbf{r}_1, ..., \mathbf{r}_N\}$. To achieve correct equilibrium and time-dependent properties, the ''boosted'' MD time step Δt_b at a given location is given by $\Delta t_b = \Delta t \exp[\beta \Delta V_b(\{\mathbf{r}_N(t)\})]$, where $\beta = 1/k_B T$, k_B is the Boltzmann constant, and T is the temperature. Since $\Delta V_b(\{\mathbf{r}_N\})$ is positive, the boosted time step is greater than Δt and the simulation can reach longer times than conventional MD. Time evolution, however, becomes a statistical property of the system and the evolved time approaches the correct value at long times.

To construct the boost potential in Voter's method, the Hessian martix $\mathscr{H}$ with components $\mathscr{H}_{ij} = \partial^2 V' / \partial x_i \partial x_j$

*Corresponding author. Tel.: +1-814-863-4807; fax: +1-814-865-7846; e-mail: kaf2@psu.edu

1385-8947/99/$ – see front matter
PII: S1385-8947(99)00055-8

needs to be calculated and diagonalized at each time step. Here x_i and x_j are components of the $3N$ dimensional vector $\mathbf{r}$. In the transition-state region, $\mathscr{H}$ has one negative eigenvalue, the gradient in potential energy vanishes [14], and the boost potential becomes zero. Although relatively efficient numerical schemes are available for calculating and diagonalizing $\mathscr{H}$, significant computational overhead is added to the simulation because of manipulations involving this matrix. Recently, Steiner et al. [15] have developed a simple boost potential in which the boosted potential energy is constant and equal to a fixed boost value if the potential energy falls below the boost value. In this method, Hessian manipulations are not performed. In this paper, we present a new boost potential which is conceptually simple, yet powerful and we demonstrate its application to surface diffusion.

2. Accelerated molecular dynamics: theory

For many systems, the average value of an observable G can be obtained with reasonable accuracy by performing a time average when the system is in equilibrium. For the canonical ensemble, where the temperature T and the number of particles N are fixed, the equilibrium average of G is expressed in terms of the phase space integrals

$$\langle G\rangle = \frac{\int\int G(\{\mathbf{r}_N\})\ \exp[-\beta K(\{\mathbf{p}_N\})]\ \exp[-\beta V(\{\mathbf{r}_N\})]\ \mathrm{d}\{\mathbf{r}_N\}\ \mathrm{d}\{\mathbf{p}_N\}}{\int\int \exp[-\beta K(\{\mathbf{p}_N\})]\ \exp[-\beta V(\{\mathbf{r}_N\})]\ \mathrm{d}\{\mathbf{p}_N\}\ \mathrm{d}\{\boldsymbol{r}_N\}}, \tag{1}$$

where $\{\mathbf{p}_N\} = \{\mathbf{p}_1, ..., \mathbf{p}_N\}$ are particle momenta and $K(\mathbf{p})$ is the kinetic energy. Using Eq. (1), the transition-state theory (TST) unimolecular rate constant from a potential-energy basin (state A) is given by the ensemble-average flux exiting through the boundary to state A [13] (Fig. 1),

$$k_{\mathrm{TST}}^{\mathrm{A}\rightarrow} = \frac{\int\int |v_{\mathrm{A}}|\delta_{\mathrm{A}}(\mathbf{r})\Theta_{\mathrm{A}}(\mathbf{r})\ \exp[-\beta K(\{\mathbf{p}_N\})]\ \exp[-\beta V(\{\mathbf{r}_N\})]\ \mathrm{d}\{\mathbf{r}_N\}\ \mathrm{d}\{\mathbf{p}_N\}}{\int\int\ \exp[-\beta K(\{\mathbf{p}_N\})]\ \exp[-\beta V(\{\mathbf{r}_N\})]\ \mathrm{d}\{\mathbf{p}_N\}\ \mathrm{d}\{\mathbf{r}_N\}}, \tag{2}$$

where $\delta_{\mathrm{A}}(\mathbf{r})$ is a Dirac delta function applicable at the boundary to state A, v_{A} is the one-dimensional velocity normal to this boundary surface, and $\Theta_{\mathrm{A}}(\mathbf{r})$ is unity when the system is in state A, and zero otherwise.

Consider Fig. 2, which shows a typical trajectory for a particle trapped in a one-dimensional potential well. The particle spends most of its time near the bottom of the well, and escapes only infrequently to an adjacent site. Significant dynamical information can be extracted only when a good sampling is obtained of trajectories near the upper portion of the well, as some of these may contribute to successful transitions to another state. Since computing trajectories near the bottom of the well consumes most of the time in traditional MD simulation of rare-event processes, the transition-state region is sampled only with significant computational effort. To improve sampling in the transition-state region, we dynamically ''heat'' the trajectories that have a lower potential energy than a fixed potential $V_{\mathrm{min}}^{\mathrm{boost}}$, as shown by a line in Fig. 2. The heating is performed in a manner that maps the particle trajectory onto a higher (''boosted'') potential-energy surface. If $S(\{\mathbf{r}_N\})$ is the boost applied to a trajectory, then the boosted potential energy of the particle is given by

$$V^*(\{\mathbf{r}_N\}) = V(\{\mathbf{r}_N\})/S(\{\mathbf{r}_N\}), \tag{3}$$

where $V(\{\mathbf{r}_N\})$ is the potential energy when no boost is applied. The boost is controlled by $S(\{\mathbf{r}_N\})$, where

$$S(\{\mathbf{r}_N\}) = 1 + f(\Delta V)\theta(\Delta V), \tag{4}$$

,$\Delta V(\{\mathbf{r}_N\}) = V_{\mathrm{min}}^{\mathrm{boost}} - V(\{\mathbf{r}_N\})$, $f\{x\}$ is a function that determines the boost, and $\theta(u)$ is the standard step function, such that θ=1 when $u \geq 0$, and θ=0 otherwise.

To ensure correct time evolution for dynamical simulations on the boosted potential-energy surface, each time step is given a weight $w(T, \{\mathbf{r}_N\})$, so that the ensemble-average escape time of Eq. (2) is correct. The weight w alters the distribution function so that the ensemble average can be calculated more efficiently [16,17]. Thus the boosted time step is given by

$$\Delta t^* = w^{-1}(T, \{\mathbf{r}_N\})\Delta t. \tag{5}$$

As in Voter's method [13], time evolves in a coarse grained manner and becomes a statistical property. Therefore, correct thermodynamic averages are obtained only in the limit of long times. Thus, using the above definitions, the TST escape rate on the boosted potential-energy surface can be written as:

$$k_{\mathrm{TST}}^{*\mathrm{A}\rightarrow} = \frac{\int\int |v_{\mathrm{A}}|\delta_{\mathrm{A}}(\mathbf{r})\Theta_{\mathrm{A}}(\mathbf{r})w^{-1}\ \exp[-\beta K(\{\mathbf{p}_N\})]\ \exp[-\beta V^*(\{\mathbf{r}_N\})]\ \mathrm{d}\{\mathbf{r}_N\}\ \mathrm{d}\{\mathbf{p}_N\}}{\int\int w^{-1}\ \exp[-\beta K(\{\mathbf{p}_N\})]\ \exp[-\beta V^*(\{\mathbf{r}_N\})]\ \mathrm{d}\{\mathbf{p}_N\}\ \mathrm{d}\{\mathbf{r}_N\}}. \tag{6}$$

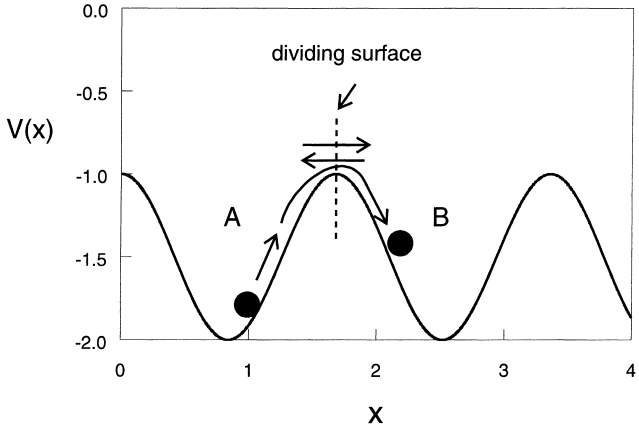

Fig. 1. The figure shows the transition of a particle from a potential energy basin (state A), to an adjacent state B. The boundary to the state A is denoted by a vertical dotted line, which forms the dividing surface.

Since the applied boost should not alter the equilibrium properties of the system, this implies

$$w^{-1}(T,\{\mathbf{r}_N\}) = \exp\left[-\beta\left(\frac{S(\{\mathbf{r}_N\})-1}{S(\{\mathbf{r}_N\})}\right)V(\{\mathbf{r}_N\})\right]. \quad (7)$$

Note that the above equation is useful as long as $V(\{\mathbf{r}_N\}) < 0$, such that $w^{-1} \geq 1$ and the boosted time step [cf., Eq. (5)] is greater than or equal to Δt. If $V(\{\mathbf{r}_N\}) > 0$, then transitions are slowed, and the method loses its utility. The condition $V(\{\mathbf{r}_N\}) < 0$, is, however, true for most condensed-phase systems. Also, as long as the function $f(x)$ [cf., Eq. (4)] is chosen judiciously, and $V_{\min}^{\text{boost}}$ is sufficiently below the transition-state energy, we can reduce any artificial effects on the transition dynamics to an adjacent state.

3. Models and method

To test and demonstrate the accelerated MD method, we have used a simple two-dimensional model, where correct results can be generated easily and accurately. To create a surface, we use a set of 70 atoms (unless otherwise mentioned), where each atom is tethered to a point which represents the starting configuration. These points are separated by a distance $1.68\sigma = \mathbf{r}_{\text{eq}}$, where $\sigma = 0.34$ nm defines a length scale. Periodic boundary conditions are applied. At a given temperature, an atom i moves away from its equilibrium tethered position, and feels a non-zero force $\mathbf{F}^{\text{spring}} = -k(\mathbf{r} - \mathbf{r}_{\text{eq}})$, where $\mathbf{r}_{\text{eq}}$ is the equilibrium position of the atom, and k is the spring constant. An adatom interacts with each of the surface atoms through the Lennard-Jones (LJ) potential

$$V_{ij}(r_{ij}) = 4\epsilon[(\sigma/r_{ij})^{12} - (\sigma/r_{ij})^{6}], \quad (8)$$

where ϵ governs the strength of the interaction, $\mathbf{r}_{ij} = \mathbf{r}_i - \mathbf{r}_j$, and $r_{ij} < r_c$. The cutoff distance for the potential is chosen as $r_c = 2.5\sigma$; beyond this distance, the potential is zero.

The dynamics of the surface atoms are described by the Langevin equation of motion, while the adatom follows Newtonian dynamics. Thus, for the surface atoms, the initial velocities are drawn from a Gaussian distribution, and then the positions and velocities are integrated for each surface particle using

$$m_i \frac{\partial \mathbf{v}_i}{\partial t} = -\xi m_i \mathbf{v}_i + \mathbf{F}_i(t) + \eta_i(t), \quad (9)$$

where ξ is the friction constant, and $\eta_i(t)$ is the delta-correlated stochastic force with zero mean. An integration routine developed by Ermak [18,19] is used to integrate the Langevin equation of motion. The friction coefficient in the simulation is chosen as $\xi = 0.5$. For the adatom, the velocity Verlet algorithm is implemented to integrate the equation of motion.

The LJ potential has been traditionally used to model liquid Argon, where the dynamics is expressed in terms of dimensionless reduced units [20]. The unit for length is σ, unit for energy is ε, and the time is expressed in the units of $\sqrt{m_{\text{ad}}\sigma^2/\epsilon}$. Here m_{ad} is the mass of the adatom. We assume that the mass for a surface atom connected by a spring, with spring constant $k = 900$ N/m, is $100m_{\text{ad}}$. By assuming the energy unit $\epsilon/k_B = 120$ K, a time step of $\Delta t = 0.00463$ in the simulation corresponds to about 10^{-14}s of real time for the adatom.

To study accelerated adatom diffusion, only the adatom is subjected to the "boost" dynamics according to Eq. (3), while the surface atoms are treated using the MD procedure described above. The function $f(\Delta V)$ that controls the adatom boost is chosen to be

$$f(\Delta V) = \frac{c\,\exp[-\gamma/\Delta V]}{1 + \exp[-\gamma/\Delta V]}, \quad (10)$$

where c and γ are tunable parameters. With this function the modified force, and potential energy are both continuous for $\lim_{\Delta V \to 0+}$. The kinetic energy (KE) and the potential energy (PE) of the whole system are monitored during the simulation for both the boosted and the un-boosted

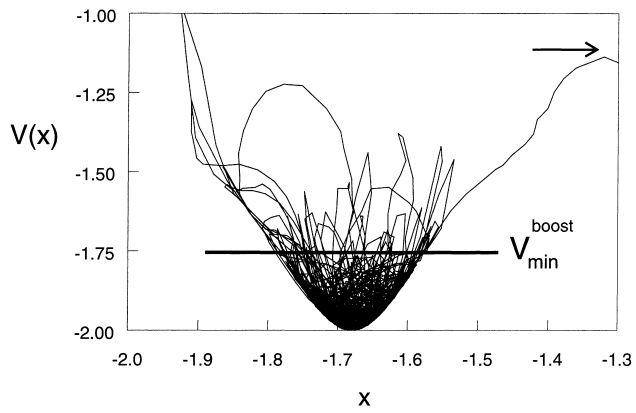

Fig. 2. A two-dimensional representation of a typical trajectory for a particle trapped in a potential well. The horizontal line denotes the value of $V_{\min}^{\text{boost}}$, below which a particle is subject to the accelerated dynamics. The arrow shows the approximate location of the potential maxima.

dynamics. In addition, the KE and the PE of the adatom are monitored to examine any sign of instability. The diffusion coefficient D is obtained from the mean-square displacement of the adatom as a function of time

$$D = \lim_{t\to\infty} \langle \frac{\Delta \boldsymbol{r}^2\rangle}{2dt}, \tag{11}$$

where $\Delta\mathbf{r}^2=[\mathbf{r}(t)-\mathbf{r}(0)]^2$, $\langle ...\rangle$ denotes ensemble average, and d is the dimensionality of the surface. We have also calculated the diffusion coefficient using the TST hopping rate. The TST rate constant k_{TST} is determined using the box-counting algorithm [17,21], which gives the TST diffusion constant $D_{\mathrm{TST}} = k_{\mathrm{TST}} l^2/2d$, where l is the hop length to adjacent binding sites.

In addition to the two-dimensional model potential described above, we have studied the diffusion of a Ag adatom on the Ag (0 0 1) surface. The MD/MC-CEM theory [22] is used to obtain the interaction energies and the forces. Once the forces are obtained for each particle via MD/MC-CEM, the positions and velocities are integrated using the velocity Verlet algorithm. A slab of 5 atoms thick in the z direction (perpendicular to the (0 0 1) surface plane), and 20 atoms wide in each of the x and y directions was chosen for the simulation. Periodic boundary conditions are applied in the x and y directions. A simulation temperature of 300 K is used and the lattice of Ag atoms are equilibrated over 100,000 time steps using $\Delta t=10^{-15}$ s, before any adatom is allowed to diffuse on the surface. As in the case of the simple two-dimensional model, only the adatom dynamics are accelerated according to Eq. (10). Also the PE, KE of the whole system, and the diffusion coefficient for the adatom are measured. Note that in this study the bias potential is defined locally, and so only the adatom is accelerated. Events that can happen outside this local region are not accelerated. This approach can corrupt the overall dynamical behavior, for example, by not accelerating events such as exchange diffusion processes. Here, however, we have chosen to follow the model defined by the local bias potential, so as to be able to draw clear comparison with previous studies [23], in which adatom hopping rates were obtained.

4. Results and discussion

To illustrate the nature of the boost acting on an adatom using Eq. (10), we have calculated the boosted potential-energy surface using Eqs. (3), (4) and (10) for a simple one-dimensional potential $V(x)=-1.205-0.1125\cos(2\pi x/1.68)$. The shapes of the surfaces for various parameters c, γ, and $V_{\mathrm{min}}^{\mathrm{boost}}$ are shown in Fig. 3. The unbiased potential is shown as a bold curve. Although, in principle, all potential energies below $V_{\mathrm{min}}^{\mathrm{boost}}$ are altered with our method, the parameters c and γ control the properties of the boost. Fig. 3(a) shows the influence of γ on the potential surface. When γ is large, the boost is conservative and the general shapes of the curves look similar to the shape of the unbiased potential-energy surface. For aggressive boosting, such as with $\gamma=0.01$, subwells are created near $V(x) = V_{\mathrm{min}}^{\mathrm{boost}}$. Although not apparent from the figures, the boosted potential-energy surfaces are continuous in the force as $\lim_{\Delta V\to 0+}$. Another way to control the boost is to vary c. Fig. 3(b) shows that larger values of c give larger boosts. As for γ, more aggressive boosting creates additional subwells in the potential-energy surface. Fig. 3(c) shows that for fixed γ and c, the shapes of the boosted potential-energy surfaces are similar, while $V_{\mathrm{min}}^{\mathrm{boost}}$ controls the amount of boost.

It should be noted that as in Voter's method, the boosted potential must be the same as the original near the transition-state region. Also, there are more subtle issues in choosing the appropriate boosting potential. The value of the diffusion coefficient can be reduced by transition-state recrossing or enhanced by long, multiple-site flights. It is known [24,25] that the extent to which these phenomena occur depends on the shape of the potential surface. The general guideline for choosing a biased potential-energy surface in the simulation is not yet well determined. However, for the reasons discussed above, we feel that the surface shapes that are not drastically different than the original potential-energy surface are good choices. For example, the biased potential with $c=0.20$, $\gamma=0.10$, and $V_{\mathrm{min}}^{\mathrm{boost}}=-1.25$ (Fig. 3(c)), which shows a flat surface, is acceptable, as it does not introduce any new subwells. However, the potential with $c=0.40$, $\gamma=0.1$, and $V_{\mathrm{min}}^{\mathrm{boost}}=-1.2$ (Fig. 3(b)) should probably be avoided, unless its effects are carefully determined for a particular application. Here we have implicitly assumed that the potential surface is stiff, i.e. the repulsive part of the potential is very steep. The function S determines the steepness of the repulsive part of the potential when a particle enters the region where $\Delta V>0$. In most applications, it is safe to have a relatively soft biased potential surface compared to the corrugation potential, since this can prevent numerical instability, reduce the influence of subwells, and limit a quick exit of a particle to an adjacent state by reflection from the biased surface.

To test the computer code and the simulation algorithm, we have simulated adatom diffusion on the two-dimensional potential surface using different time steps and temperatures. Elementary quantities such as time-averaged particle potential energy $\langle V_{\mathrm{par}}\rangle$ have been also measured for both the unbiased and biased cases. At the reduced temperature $T^*=k_{\mathrm{B}}T/\epsilon=0.07$, we get $\langle V_{\mathrm{par}}\rangle = -1.6 \pm 0.2$, by averaging over 10^6 steps. Using the same temperature, the biased particle potential energy

$$\langle V_{\mathrm{par}}^*\rangle = \frac{\sum_{i=1}^{n} w^{-1}(t_i) V_{\mathrm{par}}^*(t_i)}{\sum_{i=1}^{n} w^{-1}(t_i)}, \tag{12}$$

is -1.5 ± 0.2, where $w^{-1}(t_i)$ is given by Eq. (7), and the sum is over the number of MD steps n. For different boosts, $\langle V_{\mathrm{par}}^*\rangle$ was found to change slightly, when averaged over a

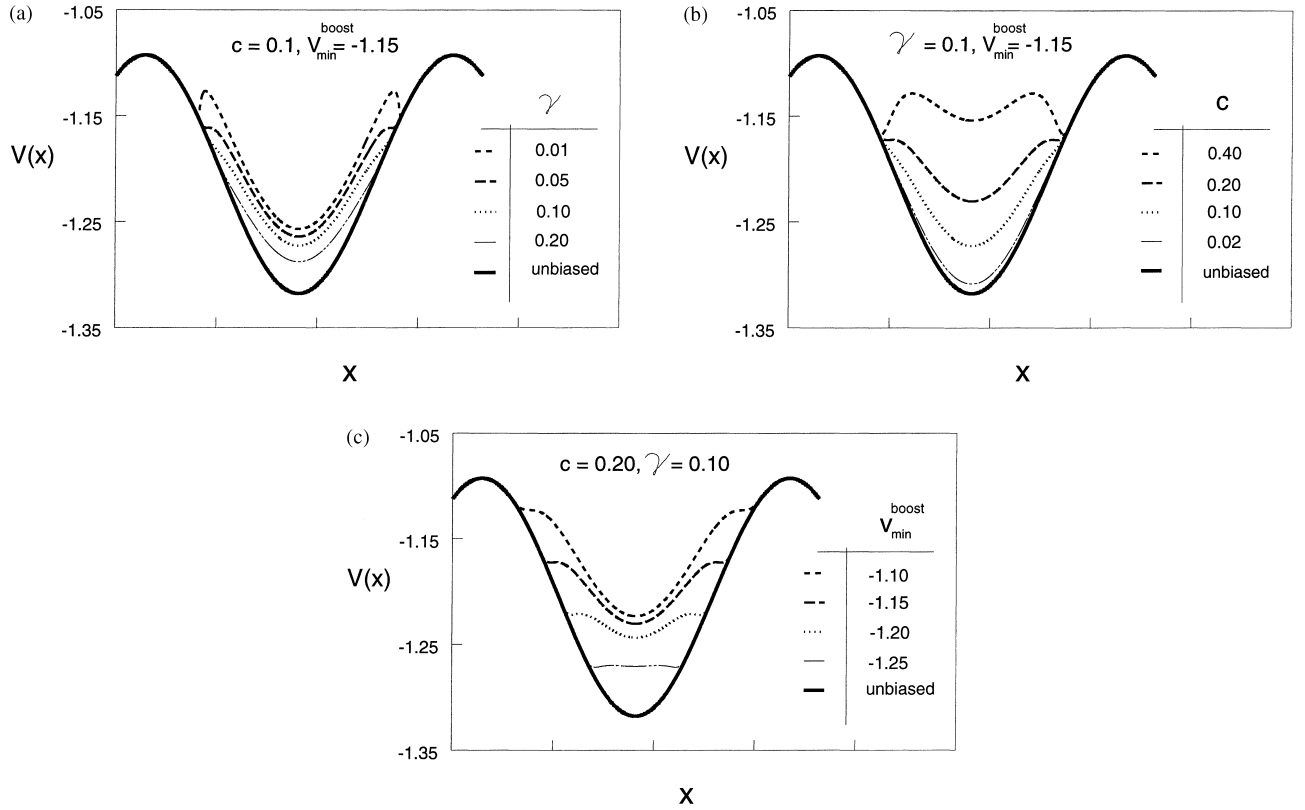

Fig. 3. (a) The biased potential-energy surface is shown for c=0.1 and $V_{\min}^{\text{boost}}$=−1.15 for different values of γ. The unbiased surface is shown as a bold curve, which obeys the equation $V(x)$=−1.205−0.1125 cos(2πx/1.68); (b) The biased potential-energy surface for various values of c, using γ=0.1 and $V_{\min}^{\text{boost}}$=−1.15. The model unbiased potential-energy surface is the same as in Fig. 3(a); (c) The change in the biased potential-energy surface is shown for various $V_{\min}^{\text{boost}}$, using c=0.2, and γ=0.1. The unbiased potential-energy surface is the same as in Fig. 3(a).

fixed time interval of 1.5×10^6 steps, showing a finite-time effect on thermodynamic averaging. Also note that due to acceleration, $\langle V_{\text{par}}^{*}\rangle$ represents averages over a much longer time than in $\langle V_{\text{par}}\rangle$. Although $\langle V_{\text{par}}\rangle = \langle V_{\text{par}}^{*}\rangle$ within statistical fluctuations, a slightly higher potential energy obtained for $\langle V_{\text{par}}^{*}\rangle$ is due to much better sampling in the transition-state region, and represents a better estimate of the particle potential energy.

In Fig. 4 we have plotted the time evolution for the adatom using a system of 100 surface atoms, at T^{*}=0.07. The y-axis shows the boosted time, while the x-axis shows the time evolution without any boost applied. A straight line fit through the data points (shown as a dotted line), gives a slope b=50.0, which represents the boost for this particular run. It should be noted that the boost achieved in a particular run not only depends on the parameters chosen for f, but also on the temperature. At lower temperatures, very large boosts to the dynamics are possible, while at higher temperatures such large boosts are no longer achievable.

Looking closely at Fig. 4, we see that the dynamics as represented by the curve, proceeds in a manner such that the boosted time t_{b} undergoes sharp jumps for small intervals in t. At other intervals, t_{b} and t advance at the same pace. When t_{b} changes fairly rapidly, the adatom is below $V_{\min}^{\text{boost}}$, and the sampling of the region where $V_{\text{par}} < V_{\min}^{\text{boost}}$ is taking place at an accelerated pace. Via this accelerated sampling, time advances much more rapidly for the accelerated MD.

To characterize the biased potential model, we have first measured the diffusion coefficient of the adatom without any boost. At the simulation temperature T^{*}=0.07, the diffusion coefficient from MD is estimated to be

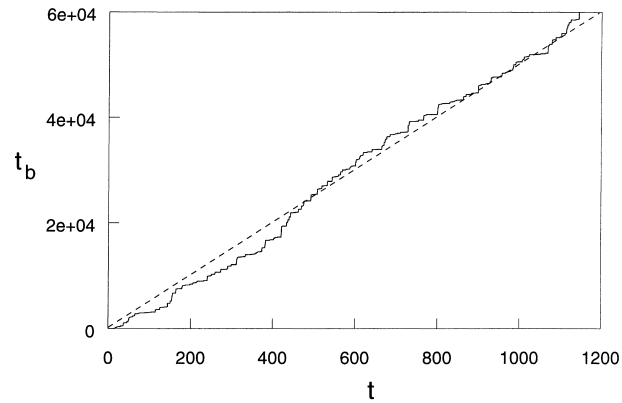

Fig. 4. A plot of boosted time t_{b} vs. the un-boosted time t in a linear scale. The boosted and un-boosted times are given as $t_b = \sum_{i=1}^{n} \Delta t_i^{*}$, and $t = \sum_{i=1}^{n} \Delta t_i$, respectively, where n is the total number of MD steps. The dotted line is a linear fit through the data points. The slope of this line gives the net boost.

Table 1

c	γ	V_{min}^{boost}	D	Boost
0.3	0.01	−1.5	$(2.1\pm0.2)\times10^{-4}$	10.2
0.3	0.008	−1.6	$(1.9\pm0.2)\times10^{-4}$	8.3
0.3	0.005	−1.8	$(2.2\pm0.2)\times10^{-4}$	4.7
0.6	0.07	−1.4	$(2.1\pm0.1)\times10^{-4}$	72.6
0.6	0.06	−1.5	$(2.0\pm0.2)\times10^{-4}$	60.8
0.6	0.07	−1.6	$(2.1\pm0.2)\times10^{-4}$	40.3
0.9	0.1	−1.4	$(2.1\pm0.1)\times10^{-4}$	299.8
0.9	0.09	−1.5	$(2.1\pm0.1)\times10^{-4}$	231.2
0.9	0.2	−1.6	$(2.2\pm0.2)\times10^{-4}$	65.6
0.9	0.2	−1.7	$(1.9\pm0.2)\times10^{-4}$	29.3

$(2.10\pm0.05)\times10^{-4}$. 40×10^6 step simulations were made, which were then averaged over 25 runs starting with new initial conditions to estimate the diffusion coefficient with reasonable accuracy. We have also estimated the diffusion coefficient using TST [17,21], which gives $D_{TST}=(2.07\pm0.02)\times10^{-4}$, a value that agrees quite well with the MD calculation.

In Table 1, we show the diffusion coefficients for various parameters and the related boost achieved using the biased potential. Each of the data points represents a simulation ranging from 9×10^6 to 15×10^6 steps, at $T^*=0.07$. The time step used is $\Delta t=0.00115$, and the diffusion coefficient D is obtained by typically sampling points over the interval of 50–100 steps, and averaging over them, after the adatom has reached the diffusive limit. The convergence of D to its long-time value can require runs of different lengths for different boost parameters. The boost depends much more strongly on c than on γ and roughly shows a 63-fold increase, with a 3-fold increase in c.

In Fig. 5 we show the shapes of the biased potential-energy surface for boosts using $c=0.3$, 0.6, and $c=0.9$, respectively (cf., Table 1.) Although subwells are visible in the figure, the dynamics (i.e., D) does not appear to be affected by them. This could be because the biased potential-energy surfaces are soft. To demonstrate this softness at the simulated temperatures, we show the trajectory of an adatom in a modified potential well with $c=0.4$, $\gamma=0.1$, and

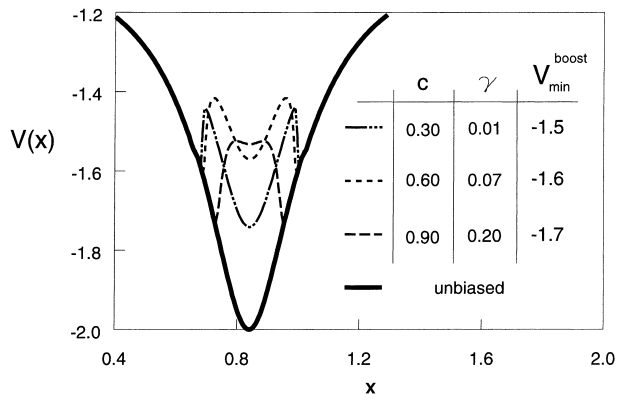

Fig. 5. Biased minimum potential-energy surfaces are shown for an adatom interacting with the surface atoms using the LJ potential.

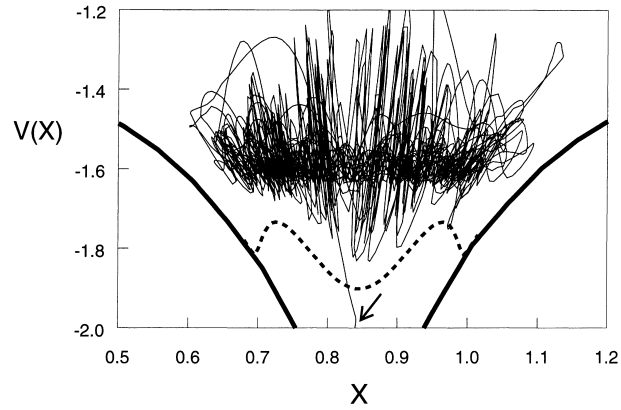

Fig. 6. The trajectory of an adatom on a biased potential-energy surface (shown as a dotted line) over 100,000 time steps. The solid line represents the unbiased potential-energy surface. These surfaces have been shifted down by a distance of 0.2 for clarity. The particle is initially located at a point indicated by the arrow. The simulation parameters are $c=0.4$, $\gamma=0.1$, $V_{min}^{boost}=-1.6$, and $T^*=0.01$. The trajectory over a much longer run appears as a uniform smear around $V_{min}^{boost}=-1.6$.

$V_{min}^{boost}=-1.6$ in Fig. 6. The adatom is initially placed at the bottom of the unbiased well, as shown by the arrow, and it is repelled to an area where its boosted potential-energy fluctuates around $V_{min}^{boost}=-1.6$. No signs of the attractive subwells are seen at this temperature. Under such a scenario, it appears that the stiffness of the biased potential-energy surface is an important quantity as well, and should be used to characterize the biased surface.

We have used accelerated MD to study adatom diffusion on the Ag(0 0 1) surface using CEM. Fig. 7 shows the corrugation potential of the unbiased surface with minimum

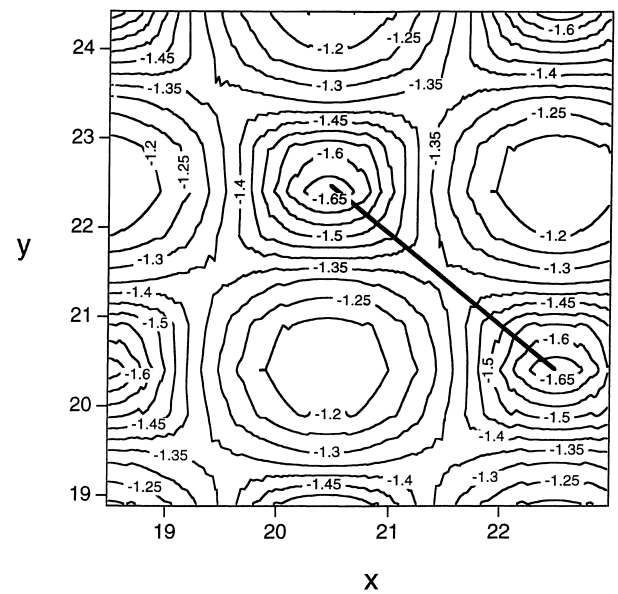

Fig. 7. Contour plot of the corrugation potential for the Ag (0 0 1) surface is shown. The line shows the minimum-energy pathway from one potential-energy minimum to another. The energy barrier between these two minima is 0.25 eV [23].

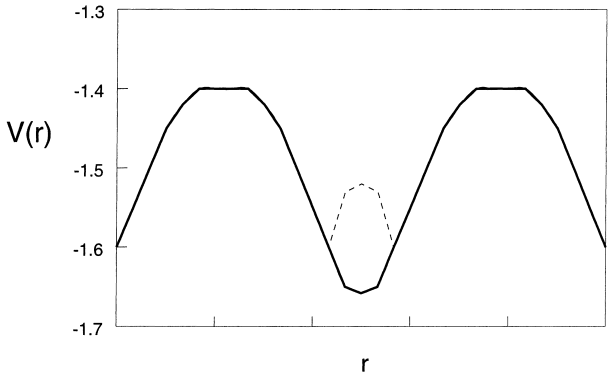

Fig. 8. The variation of potential energy (in eV) along the minimum-energy pathway is shown by the bold curve for the Ag (0 0 1) surface. The dotted line represents the biased potential-energy surface using c=0.30, γ=0.03, and $V_{\min}^{\text{boost}}=-1.6$.

potential energy ~ -1.67 eV and the maximum ~ -1.15 eV. The line shows the minimum-energy pathway with barrier of 0.25 eV [23]. The variation of the potential energy along the line in Fig. 7 is shown in Fig. 8 by a bold curve. The boosted potential-energy surface, characterized by c=0.3, γ=0.03, and $V_{\min}^{\text{boost}}=-1.6$, is shown by the dotted curve in Fig. 8. On the un-biased surface, MD simulations yield a diffusion coefficient $D\sim 9.4\times 10^{-8}$ cm^2/s at 300 K [23]. A 20,000 step MD run was made to estimate the diffusion coefficient at 300 K. Using the boosted potential shown in Fig. 8, we get D from the accelerated MD as $(10\pm 3)\times 10^{-8}$cm^2/s, with a boost of b=375. This exemplifies the great potential of accelerated MD for enhancing our ability to study rare-event dynamics.

5. Summary and conclusions

We have presented a new MD method for studying the dynamics of infrequent events. The method accelerates sampling in the transition-state region by dynamically heating the trajectories. A boost function S is used for this purpose, which raises the potential-energy surface in regions of phase space, where normally traditional MD calculations would spend most time, thus enabling significant acceleration. Since the dynamics should be independent of the choice of the function S, more study is needed to ascertain if a universal boost function can be determined.

Our elementary results for the study of adatom diffusion on a two-dimensional potential surface and on a three-dimensional Ag(0 0 1) potential-energy surface demonstrate the viability and power of this method. Significant boosts can be achieved in the dynamical evolution, where similar studies using the traditional MD procedure can take days to months of computer time.

This research is supported by NSF grant DMR-9617122.

References

[1] A.F. Voter, Phys. Rev. B 34 (1986) 6819.
[2] H.C. Kang, W.H. Weinberg, J. Chem. Phys. 90 (1989) 2824.
[3] K.A. Fichthorn, W.H. Weinberg, J. Chem. Phys. 95 (1991) 1090.
[4] E.J. Dawnkaski, D. Srivastava, B.J. Garrison, Chem. Phys. Lett. 232 (1995) 524.
[5] H. Metiu, Y.-T. Lu, Z. Zhang, Science 255 (1992) 1088.
[6] R. Marcelin, Ann. Phys. 3 (1915) 120.
[7] E. Wigner, Z. Phys. Chem. B 19 (1932) 203.
[8] H. Eyring, J. Chem. Phys. 3 (1935) 107.
[9] L. Monnerie, U.W. Suter, Adv. Polym. Sci. 116 (1994) 207.
[10] D.N. Theodorou, in: I.C. Sanchez (Ed.), Physics of Polymer Surfaces and Interfaces, Butterworth-Heinemann, Boston, 1992, p. 139.
[11] F. Lancon, L. Billard, W. Chambron, A. Chamberod, J. Phys. F: Met. Phys. 15 (1985) 1485.
[12] P.E. Blöchl, C.G. Van de Walle, S.T. Pantelides, Phys. Rev. Lett. 64 (1990) 1401.
[13] A.F. Voter, J. Chem. Phys. 106 (1997) 4665.
[14] E.M. Sevick, A.T. Bell, D.N. Theodorou, J. Chem. Phys. 98 (1993) 3196.
[15] M.M. Steiner, P.-A. Genilloud, J.W. Wilkins, Phys. Rev. B 57 (1998) 10236.
[16] N. Metropolis, A. Rosenbluth, M. Rosenbluth, M. Teller, E. Teller, J. Chem. Phys. 21 (1953) 1087.
[17] A.F. Voter, J.D. Doll, J. Chem. Phys. 80 (1984) 5814.
[18] M.P. Allen, D.J. Tildesly, Computer Simulation of Liquids, Oxford University Press, Oxford, 1987.
[19] D.L. Ermak, H. Buckholtz, J. Comput. Phys. 35 (1980) 169.
[20] A. Rahman, Phys. Rev. A 136 (1964) 405.
[21] A.F. Voter, J. Chem. Phys. 82 (1985) 1890.
[22] M.S. Stave, D.E. Sanders, T.J. Raeker, A.E. DePristo, J. Chem. Phys. 93 (1990) 4413.
[23] D.E. Sanders, A.E. DePristo, Surf. Sci. 260 (1992) 116.
[24] D.E. Sanders, A.E. DePristo, Surf. Sci. Lett. 264 (1992) 169.
[25] J.M. Cohen, A.F. Voter, Surf. Sci. 313 (1994) 439.